Fourier-Bessel series expansion based blind deconvolution method for bearing fault detection

E. Soave[1], **G. D'Elia**[1], **G. Dalpiaz**[1]
[1]University of Ferrara, Department of Mechanical Engineering,
via Saragat 1, 44122 Ferrara, Italy
e-mail: elia.soave@unife.it

Abstract

In the last few years blind deconvolution techniques proved to be useful in order to extract impulsive patterns related to bearing fault from noisy vibration signals. Recently, a novel blind deconvolution method based on the generalized Rayleigh quotient has been proposed and an iterative algorithm related to the maximization of the cyclostationarity of the source has been defined. This paper presents a new condition indicator that exploit the Fourier-Bessel series expansion for the computation of a new cyclostationarity index that drives the maximization problem for the extraction of the excitation source. The main target of this work is to compare the results obtained through the exploitation of the Fourier-Bessel transform with respect to the classic Fourier transform in term of lower number of cyclic frequencies required for the algorithm. The comparison between the application of the two different methods involves both simulated and real signal taking into account a bearing fault. The results prove the capability of the new indicator to extract the impulsive source without the need of a set of cyclic frequencies but only with the first one, with a strong reduction of the computational time.

Keyword: Cyclostationarity, Fourier-Bessel transform, blind deconvolution, bearing fault detection.

1 Introduction

Nowadays, bearing fault detection and identification play a fundamental role in the diagnostics of rotating machines being this component one of the most critical in mechanical systems. However, the detection of bearing faults, particularly in the first stage of the damaging process, may be challenging due to the fact that the impulsive pattern related to the fault is very weak and consequently masked by the background noise and other interference. For this purpose, blind deconvolution (BD) techniques proved to be able to extract the characteristic impulsive pattern of a faulty bearing direct from a noisy observation, under the hypothesis of linear time-invariant system.

The first BD method, called Minimum Entropy Deconvolution (MED) [1], exploits an iterative algorithm in order to extract the impulsive source through the maximization of the kurtosis directly from a noisy vibration signal convolved with an unknown impulse response function. Over the years, the MED algorithm has been exploited for machine diagnosis by many authors both for tooth faults [2, 3] and bearing faults [4] in combination with other signal processing techniques. However, from the machine diagnosis point of view kurtosis can not be considered a a useful indicator. In fact, this statistics is sensitive to signal with a single peak rather than to signal peakedness according to a given periodicity, e.g. represented by a train of impulses.

In order to overcome this problem and exploit the BD for the fault detection in rotating machines, McDonald at al. [5] proposed a new BD method based on a criterion called correlated kurtosis that is sensitive to signal composed by a train of periodic peaks. This algorithm, called Maximum Correlated Kurtosis Deconvolution (MCKD), is based on an iterative process that aims to estimate the source having the maximum correlated kurtosis.

In the same direction, McDonald and Zhao [6] proposed a new BD method called Multipoint Optimal Minimum Entropy Deconvolution Adjusted (MOMEDA). This direct algorithm promotes the estimation of a

pattern of periodic impulses by considering a target vector **t**, defined as a train of equispaced impulses. The main issue of MOMEDA is related to the definition of **t** that allows the extraction of periodic impulses.

Over the years, cyclostationarity proved to be effective for machine diagnosis. In particular, several works [7, 8] prove that the vibration signal related to a bearing fault is not strictly periodic due to a random "jitter" around the fault period, but it can be seen as a second order cyclostationary signal. The correlated kurtosis can be seen as a cyclostationary criterion being it related to the autocorrelation function of the instantaneous power of the signal [9]. However, it has been defined empirically, without an explicit formulation regarding it cyclostationary nature, thus there is the need to define a pure cyclostationary criterion.

Recently, in this direction, Buzzoni et al. [10] proposed a new BD method based on the maximization of the cyclostationarity of the researched signal through an iterative algorithm that solves an eigenvalue problem starting from a generalized Rayleigh quotient. This algorithm aims to extract the source related to the maximum value of the Indicator of Ciclostationarity (ICS). This indicator, proposed for the first time by Raad et al. [11], exploits the Fourier transform in order to extract the hidden periodicity inside the acquired signal. However, the Fourier series expansion requires an high number of terms for the description of an impulsive pattern. For this reason, the algorithm needs to take account of a certain number of harmonics of the cyclic frequency related to the investigated periodicity in order to reach a sufficient reconstruction quality.

The target of this work is the definition of a new BD indicator based on the maximization of the ciclostationary behavior of the analyzed signal. This indicator exploits the Fourier-Bessel series expansion instead of the classical Fourier transform. The choice of this particular series expansion is related to the fact that, unlike the sinusoidal function based Fourier transform, it is based on the Bessel functions that quickly decay according to a specific law [12, 13]. For this reason, the proposed method requires a set of cyclic frequencies with a lower number of harmonics, strongly reducing the computational time of the iterative algorithm.

The BD method modified through the exploitation of a new indicator is verified through the analysis of both simulated signal and a real test case in order to demonstrate its effectiveness for the fault detection and the condition monitoring of bearings. The comparison between the proposed method and the other methods based on the ciclostationarity maximization aims to point out the improvement given by the proposed algorithm, in particular in term of computational time reduction.

2 Overview about blind deconvolution methods through generalized Rayleigh quotient optimization

The target of BD is the extraction of an input signal, typically related to the excitation given by a fault, directly from a noisy observation under the hypothesis of linear time invariant system.

The vibration signal, from now called **x**, can be considered as composed by three different parts: an impulsive pattern $\mathbf{s}_0$ related to a local fault, a periodic component **p** and a Gaussian background noise **n**, all convolved with their respective Impulse Response Function (IRF), viz:

$$\mathbf{x} = \mathbf{s}_0 * \mathbf{g}_s + \mathbf{p} * \mathbf{g}_p + \mathbf{n} * \mathbf{g}_n \tag{1}$$

where $\mathbf{g}_s$, $\mathbf{g}_p$ and $\mathbf{g}_n$ are the IRFs related to $\mathbf{s}_0$, **p** and **n**, respectively and * refers to the convolution operation.

BD aims to estimate an inverse filter **h** (assumed to be a FIR filter) in order to deconvolve the excitation $\mathbf{s}_0$ from **x** minimizing the other contributions, such that:

$$\mathbf{s} = \mathbf{x} * \mathbf{h} = (\mathbf{s}_0 * \mathbf{g}_s + \mathbf{p} * \mathbf{g}_p + \mathbf{n} * \mathbf{g}_n) * \mathbf{h} \approx \mathbf{s}_0 \tag{2}$$

In the first part of eq. 2 the convolution can be expressed for discrete signals in matrix form, as follow:

$$\mathbf{s} = \mathbf{X}\mathbf{h} \tag{3a}$$

$$\begin{bmatrix} s[0] \\ \vdots \\ s[L-1] \end{bmatrix} = \begin{bmatrix} x[N-1] & \dots & x[0] \\ \vdots & \ddots & \vdots \\ x[L-1] & \dots & x[L-N-2] \end{bmatrix} \begin{bmatrix} h[0] \\ \vdots \\ h[N-1] \end{bmatrix} \tag{3b}$$

where L and N are the number of samples of **s** and **h**, respectively. The main problem is related to the fact that the IRFs described in eq. 2 are not available. A possible solution can be achieved considering an arbitrary

criterion based on a priori assumption, e.g. assuming that a statistical property is maximized by the researched source. Thus, BD aims to recover the source that maximizes a certain statistical property, e.g. kurtosis [1], correlated kurtosis [5] or multi D-Norm [6], through iterative or direct algorithms.

Although cyclostationarity plays a fundamental role in the diagnostics of rolling element bearings the CYCBD method [10] can be considered as the first BD method that exploits the cyclostationary signature of faulty bearings.

2.1 Blind deconvolution algorithms driven by cyclostationarity maximization based on generalized Rayleigh quotient

Recently, the method proposed in Ref. [10] demonstrated that the generalized Rayleigh quotient can be exploited in order to define a new optimization problem. Starting from this statement a new BD method based on the cyclostationarity maximization has been defined.

A generical process can be defined as cyclostationary if its statistical properties exhibit a periodic behaviour. It has been demonstrated by several authors [7, 8] that the vibration signature related to a faulty bearing shows a cyclostationary behavior, thus this property became pivotal for bearing fault detection and identification. In this scenario, the frequency related to the periodic behavior of any statistic of the process is called cyclic frequency and, for discrete signal, can be expressed as follow:

$$\alpha = \frac{k}{T} \tag{4}$$

where k is the sample index and T the cyclic period, e.g. the characteristic period of a bearing fault. The BD algorithm descried in this section, called CYCBD, is based on the maximization of the second-order ICS that describes the presence of periodic fluctuations of the energy flow of the signal.

First of all, it is necessary to remember the definition of second-order ICS:

$$ICS_2 = \frac{\sum\limits_{k>0} |c_s^k|^2}{|c_s^0|^2} \tag{5}$$

with

$$c_s^k = \frac{1}{L-N+1} \sum_{n=N-1}^{L-1} |s[n]|^2 e^{-j2\pi \frac{k}{T} n} \tag{6a}$$

$$c_s^0 = \frac{||\mathbf{s}||^2}{L-N+1} \tag{6b}$$

or, in matrix form:

$$c_s^k = \frac{\mathbf{E}^H |\mathbf{s}|^2}{L-N+1} \tag{7a}$$

$$c_s^0 = \frac{\mathbf{s}^H \mathbf{s}}{L-N+1} \tag{7b}$$

where

$$|\mathbf{s}|^2 = [|s[N-1]|^2, \ldots, |s[L-1]|^2]^T \tag{8a}$$

$$\mathbf{E} = \begin{bmatrix} e^{-j2\pi \frac{1}{T}(N-1)} & \ldots & e^{-j2\pi \frac{K}{T}(N-1)} \\ \vdots & \ddots & \vdots \\ e^{-j2\pi \frac{1}{T}(L-1)} & \ldots & e^{-j2\pi \frac{K}{T}(L-1)} \end{bmatrix} \tag{8b}$$

Now it is possible to rewrite eq. 5 by substituting eq. 7a and 7b as:

$$ICS_2 = \frac{|\mathbf{s}|^{2H} \mathbf{E}\mathbf{E}^H |\mathbf{s}|^2}{|\mathbf{s}^H \mathbf{s}|^2} \tag{9}$$

Finally, ICS_2 can be rewritten by substituting eq. 3a into eq. 9, viz:

$$ICS_2 = \frac{\mathbf{h}^H \mathbf{X}^H \mathbf{W} \mathbf{X} \mathbf{h}}{\mathbf{h}^H \mathbf{X}^H \mathbf{X} \mathbf{h}} = \frac{\mathbf{h}^H \mathbf{R}_{XWX} \mathbf{h}}{\mathbf{h}^H \mathbf{R}_{XX} \mathbf{h}} \tag{10}$$

where $\mathbf{R}_{XWX}$ and $\mathbf{R}_{XX}$ are the weighted correlation matrix and the correlation matrix, respectively, and $\mathbf{W}$ is the weighting matrix, expressed as:

$$\mathbf{W} = diag\Big(\frac{\mathbf{E}\mathbf{E}^H|\mathbf{s}|^2}{(L-N+1)\mathbf{s}^H\mathbf{s}}\Big)(L-N+1) = \begin{bmatrix} \ddots & & 0 \\ & \frac{\mathbf{E}\mathbf{E}^H|\mathbf{s}|^2}{(L-N+1)} & \\ 0 & & \ddots \end{bmatrix} \frac{(L-N+1)}{\sum_{n=N-1}^{L-1} s[n]^2} \tag{11}$$

It should be noticed that eq. 10 is a generalized Rayleigh quotient. It has been demonstrated [10] that the maximization of the ICS_2 in eq. 10 with respect to the filter coefficients $\mathbf{h}$ is equivalent to the eigenvector related to the maximum eigenvalue λ of the following generalized eigenvalue problem:

$$\mathbf{R}_{XWX}\mathbf{h} = \mathbf{R}_{XX}\mathbf{h}\lambda \tag{12}$$

thus, the maximum value of λ correspond to the maximum value of ICS_2.

The maximization of ICS_2 and the extraction of the associated filter $\mathbf{h}$ is reached through an iterative process. The iteration starts with an initialization of the inverse filter $\mathbf{h}$ in order to compute the weighting matrix $\mathbf{W}$ and solve the eigenvalue problem described in eq. 12, obtaining the filter $\mathbf{h}$ related to the maximum value of λ. The iterative process restarts from the evaluation of $\mathbf{W}$ and goes on until convergence. A suitable solution for the computation of a guess of $\mathbf{h}$ is to estimate the filter coefficient through an auto-regressive (AR) model filter, e.g. by means of the Yule-Walker equations, according to Ref. [10]. This model permits to attenuate all the components related to deterministic sources in the signal spectra thus it is possible to obtain a flat spectral density, typical of a impulsive patterns.

Once the iterative process is ended, the maximum value of ICS_2 is available and the source obtained by substituting the related value of $\mathbf{h}$ into eq. 3a represents the final deconvolved source.

3 Fourier-Bessel series expansion based blind deconvolution method

3.1 Fourier-Bessel series expansion

Let us consider a generic discrete signal x(n); the Fourier-Bessel series expansion can be written in the discrete form as follows:

$$x(n) = \sum_{i=1}^{L} C_i J_0\Big(\frac{\beta_i n}{L}\Big), n = 0, 1, ..., L-1 \tag{13}$$

where L is the length of x, J_0 is the zero-order Bessel function and C_i are the Fourier-Bessel series coefficients, defined as:

$$C_i = \frac{2}{L^2[J_1(\beta_i)]^2} \sum_{n=0}^{L-1} n x(n) J_0\Big(\frac{\beta_i n}{L}\Big) \tag{14}$$

where J_1 is the first order Bessel function and β_i are the positive roots of $J_0 = 0$.

According to Schroeder [14], the positive roots of the zero order Bessel function are related to the frequency domain by the following:

$$\beta_i \approx \frac{2\pi f_i L}{f_s} \tag{15}$$

where f_s is the sampling frequency of x(n).

It is possible to compare the Fourier-Bessel coefficients C_i with the Fourier coefficients for the description of the signal x(n). However, the Bessel functions decay within the range defined by L according to eq. 13, instead of the sinusoidal functions on which is based the Fourier series. For this reason, the Fourier-Bessel transform requires a lower number of coefficients, with respect to the classic Fourier transform, in order to obtain high quality in the reconstruction of the signal.

This work aims to exploit this characteristic of the Fourier-Bessel transform in order to define a new BD criterion that permits the reduction of the computational time of the iterative algorithm due to the lower number of cyclic frequency harmonics required for the analysis.

3.2 Proposed method

The CYCBD algorithm can be reformulated as follows. First of all, let us remember the second order indicator of ciclostationarity defined in eq. 5. Unlike the formula described in eq. 6, the numerator of the ICS_2 can be rewritten exploiting the Fourier-Bessel series expansion described in eq. 14 as follows:

$$c_F^k = \frac{2}{(L-N+1)^2[J_1(\beta_k)]^2} \sum_{n=N-1}^{L-1} n|s(n)|^2 J_0\Big(\frac{\beta_k n}{L-N+1}\Big) \tag{16}$$

where the roots of the zero-order Bessel function can be expressed as:

$$\beta_k = \frac{2\pi \frac{k}{T_s}(L-N+1)}{f_s} \tag{17}$$

where the term k/T_s represents the cyclic frequency, according to eq. 4.

Eq. 16 can be expressed in matrix form as follows:

$$c_F^k = \frac{2}{(L-N+1)^2} \frac{\mathbf{J}_{0_n}^H |\mathbf{s}|^2}{\mathbf{J}_1 \mathbf{J}_1^H} \tag{18}$$

where

$$|\mathbf{s}|^2 = [|s[N-1]|^2, \ldots, |s[L-1]|^2]^T \tag{19a}$$

$$\mathbf{J}_{0_n} = \begin{bmatrix} J_0\Big(\frac{\beta_1(N-1)}{L-N+1}\Big)(N-1) & \ldots & J_0\Big(\frac{\beta_K(N-1)}{L-N+1}\Big)(N-1) \\ \vdots & \ddots & \vdots \\ J_0\Big(\frac{\beta_1(L-1)}{L-N+1}\Big)(L-1) & \ldots & J_0\Big(\frac{\beta_K(L-1)}{L-N+1}\Big)(L-1) \end{bmatrix} \tag{19b}$$

$$\mathbf{J}_1 = [J_1(\beta_1) \ldots J_1(\beta_k) \ldots J_1(\beta_K)] \tag{19c}$$

Starting from eq. 7b and eq. 18, eq. 5 can be rewritten as:

$$ICS_{2F} = \frac{4}{(L-N+1)^2 |\mathbf{J}_1 \mathbf{J}_1^H|^2} \frac{|\mathbf{s}|^{2H} \mathbf{J}_{0_n} \mathbf{J}_{0_n}^H |\mathbf{s}|^2}{|\mathbf{s}^H \mathbf{s}|^2} \tag{20}$$

Analogously to the CYCBD method, it is possible to note that all the periodic components of $|\mathbf{s}|^2$ are comprising into the following signal:

$$P[\mathbf{s}] = \frac{4}{(L-N+1)^2} \sum_{k>0} \frac{J_{0_n}^k (J_{0_n}^k |s|^2)}{[J_1(\beta_k)]^2} = \frac{4}{(L-N+1)^2} \frac{\mathbf{J}_{0_n} \mathbf{J}_{0_n}^H |\mathbf{s}|^2}{|\mathbf{J}_1 \mathbf{J}_1^H|^2} \tag{21}$$

Substituting eq. 3a and eq. 21 into eq. 20 it is possible to write the ICS_2 as a generalized Rayleigh quotient:

$$ICS_{2F} = \frac{\mathbf{h}^H \mathbf{X}^H \mathbf{W} \mathbf{X} \mathbf{h}}{\mathbf{h}^H \mathbf{X}^H \mathbf{X} \mathbf{h}} = \frac{\mathbf{h}^H \mathbf{R}_{XWX} \mathbf{h}}{\mathbf{h}^H \mathbf{R}_{XX} \mathbf{h}} \tag{22}$$

where the weighting matrix can be expressed as:

$$\mathbf{W} = diag\Big(\frac{P[|\mathbf{s}|^2]}{\mathbf{s}^H \mathbf{s}}\Big)(L-N+1) = \begin{bmatrix} \ddots & & 0 \\ & P[|\mathbf{s}|^2] & \\ 0 & & \ddots \end{bmatrix} \frac{1}{\sum_{n=N-1}^{L-1} s[n]^2} \tag{23}$$

Eq. 22 is the base of the proposed BD method, called Fourier-Bessel Blind Deconvolution (FBBD). The maximum value of the proposed criterion can be found by solving the same iterative process based on the maximization of the Rayleigh quotient described in section 2.1.

4 Application to simulated signal

The FBBD method proposed in the previous section has been validated taking into account a simulated signal that reproduces a characteristic cyclostationary signal. During the validation the method is compared with the CYCBD method described in section 2 in order to demonstrate the improvement given by the Fourier-Bessel transform, specially in term of lower computational time due to the lower number of cyclic frequencies required by the algorithm.

4.1 Simulated signal

The simulated signal used for the validation of the proposed method has been created according to eq. 1, neglecting the periodic pattern **p** as follows:

$$\mathbf{x} = \mathbf{s}_0 * \mathbf{g}_s + \mathbf{n} * \mathbf{g}_n \tag{24}$$

where the IRFs $\mathbf{g}_s$ and $\mathbf{g}_n$ have been defined according to the model of the response of a damped single degree of freedom (SDOF) system to a unit impulse in the time domain. For continuous signal, this IRF can be defined in term of displacement as:

$$\mathbf{x}_{SDOF} = Ae^{-\zeta\omega_n t} sin(\omega_d t) \tag{25}$$

where A is the response amplitude, ζ is the damping coefficient, ω_n is the resonance frequency and ω_d is given by the following:

$$\omega_d = \omega_n \sqrt{1-\zeta^2} \tag{26}$$

Starting from eq. 25 the IRFs can be defined in term of acceleration by taking the second derivative with respect to the time.

Table 1: Parameters used for the IRFs.

	$\mathbf{g}_s$	$\mathbf{g}_n$
A	1.810^{-10}	1.210^{-10}
ζ	0.005	0.045
ω_n(rad/s)	18.84	62.83

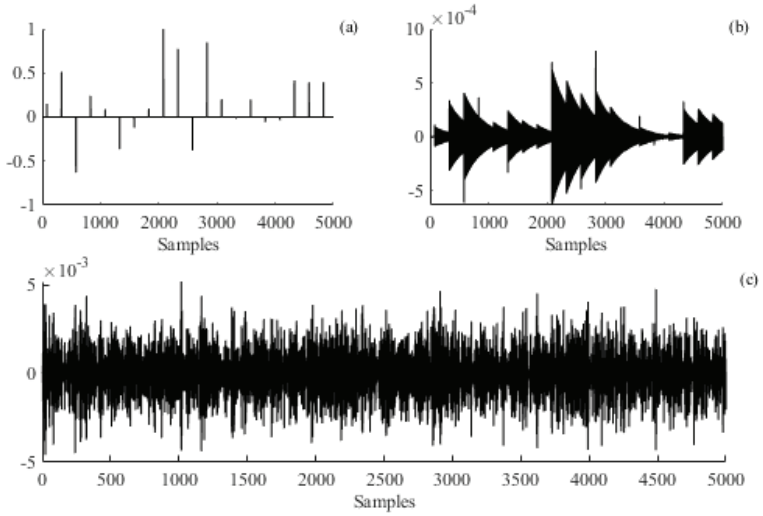

Figure 1: Simulated signal used for the validation: impulsive pattern with Gaussian distributed amplitudes (a), impulsive pattern convolved with its IRF (b) and overall signal (c).

The cyclostationary signal used for the validation is composed by a pattern of periodic impulses (with 250 samples period) with amplitudes distributed according to a Gaussian law and an additive Gaussian background noise (SNR = -17dB). The IRFs $\mathbf{g}_s$ and $\mathbf{g}_n$ are described by the parameters collected in table 1.

Figure 1 depicts the overall simulated signal and the patterns that compose it. It is possible to note that in the overall signal the periodic impulses are strongly masked by the background noise. For this reason the extraction of the cyclostationary source may represent a challenging test for the proposed method thus this validation may permit to demonstrate the effectiveness of the FBBD algorithm.

4.2 Results

The simulated signal has been analyzed through FBBD and CYCBD method in order to highlight the improvement given by the proposed algorithm, in particular in term of lower number of cyclic frequencies required. Due to the inability of BD methods to find the real amplitude of the researched pattern, all the sources obtained from the analysis has been normalized by their respective maximum value.

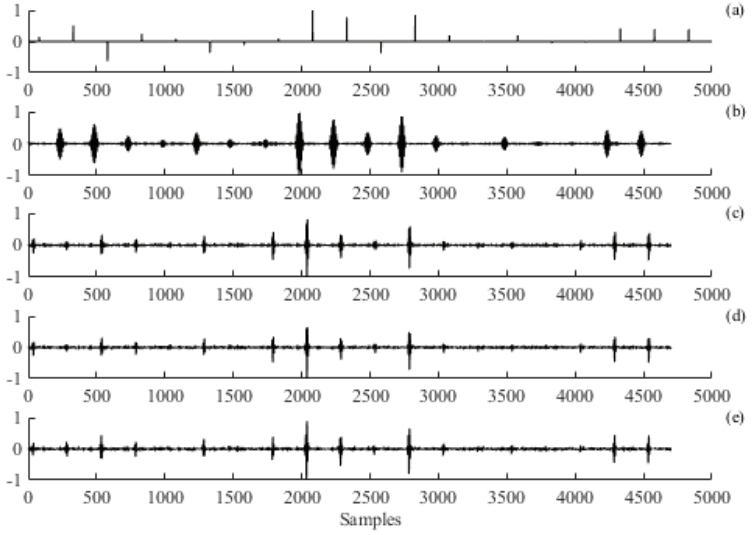

Figure 2: Comparison between the target source (a) and the patterns estimated through the FBBD method at increasing number of cyclic frequencies (from b to e).

Figure 2 reports the results obtained through the application of the FBBD method considering an increasing number of cyclic frequency harmonics, i.e. 1, 10, 30, 50 (from top to bottom). It clearly shows that the FBBD is able to extract the impulsive pattern with the same period of the target source and with the correct relative amplitudes. It has to be underlined that the deconvolved source presents a delay with respect the reference signal, due to the filtering operation inside the BD algorithm. However, this delay does not influence the results thus it is not corrected in the following analysis.

The main issue pointed out by the comparison between the estimated sources and the target pattern is related to the sign of the recovered impulses. In fact, it has to be noticed that the FBBD algorithm is not able to recover the correct sign of the impulses but it extracts a source composed by symmetric peaks. This particular behaviour do not depend on the number of cyclic frequencies used for the analysis. In fact, comparing the sources in figure 2(c to e) it is possible to see no changing in the reconstructed signal amplitudes with increasing number of cyclic frequency harmonics. This result agrees with the consideration explained in section 3 about the low number of term required by the Fourier-Bessel transform for the reconstruction of signal with sufficient quality.

Figure 3 depicts the sources estimated after the application of the CYCBD algorithm at increasing number of considered cyclic frequency harmonics, i.e. 10, 30, 50, 100 (from b to e). There is a significant difference between the behaviour of the CYCBD and the FBBD for different number of considered harmonics. For low number of cyclic frequency harmonics, i.e. 10 as shown in figure 3(b), the estimated source is not able to reproduce the real sign of the impulses as well as for the FBBD method. However, considering an higher

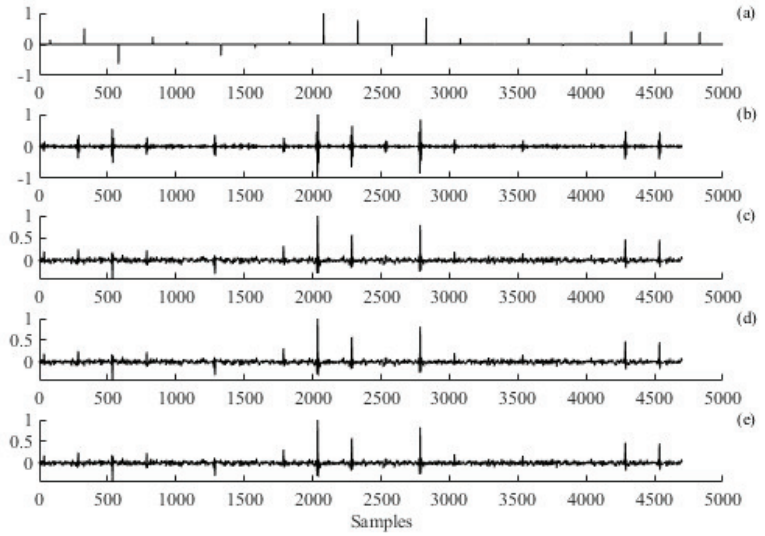

Figure 3: Comparison between the target source (a) and the patterns estimated through the CYCBD method at increasing number of cyclic frequencies (from b to e).

number of cyclic frequency harmonics, i.e. 30, 50 and 100 as shown in figure 3(c-e), the algorithm permits to extract the correct sign of the peaks, reproducing the target source with higher quality with respect to the FBBD algorithm.

Moreover, comparing figure 3(b-e) it has to be noticed that the quality of the reconstruction reaches an acceptable level considering at least 30 cyclic frequency harmonics (figure 3(c)). Further increasing the number of harmonics (figure 3(d-e)), the deconvolved source does not seem to present any improvement from this point of view.

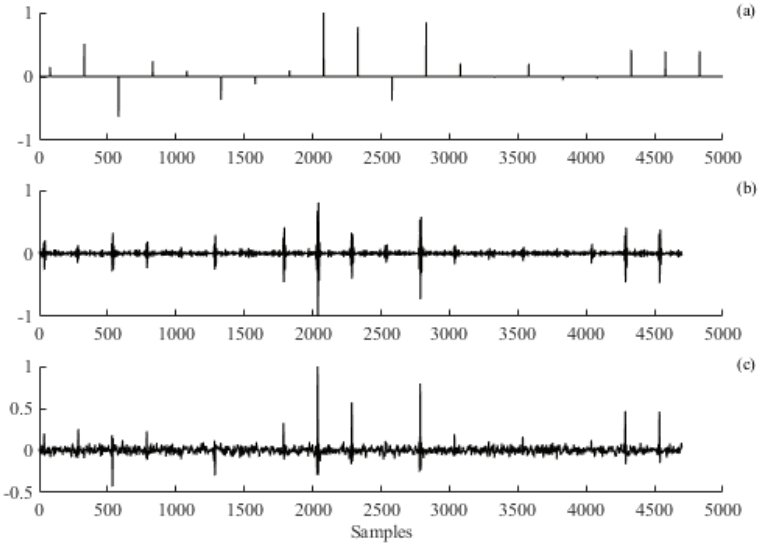

Figure 4: Comparison between the target source (a) and the sources estimated through the FBBD method (b) and the CYCBD method (c).

Figure 4 compares the impulsive patterns recovered using both FBBD and CYCBD. All two methods has been applied using the minimum number of cyclic frequency harmonics identified by the previous analysis, i.e. 10 and 30 respectively.

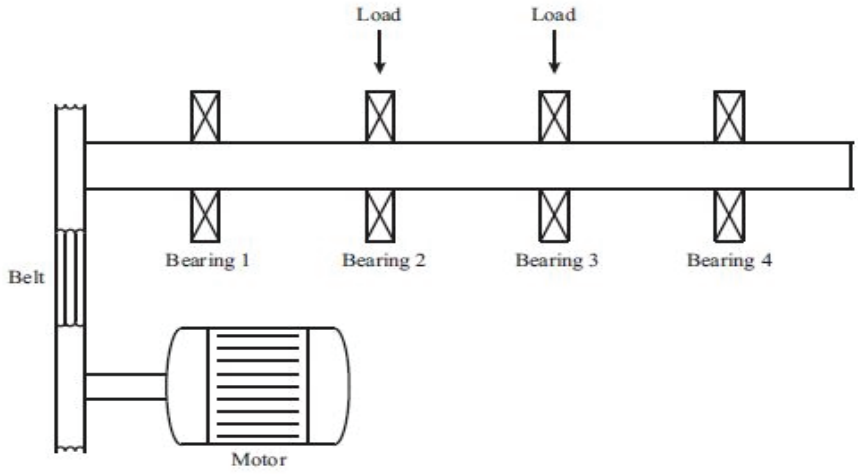

Figure 5: Scheme of the experimental test rig.

The comparison clearly underlines the main difference between the results obtained applying the two methods, represented by the gap in term of reconstruction of the correct sign of the source. In fact, as already seen in figure 2 the FBBD extracts a zero mean impulsive pattern, independently from the real sign of the peaks. However, this issue may be considered irrelevant for diagnostics purposes where the main attention is pointed out on the frequency of the impulses instead of their amplitudes. On the other hand, the FBBD seems to permit the identification of the lower amplitude impulses better tha the CYCBD. For examples, comparing figures 4(b-c) it can be seen that the impulses close to 2500 and 4000 samples are clearly identified only by the FBBD, due to the higher amplitude of the noise in the source deconvolved by the CYCBD that masks these peaks.

These results, combined with the lower number of cyclic frequencies required (70% less), demonstrates the clear improvement given by the FBBD method for the extraction of hidden ciclostationary pattern directly from noisy observations such as the characteristic vibration signal related to faulty bearings.

5 Application to real signal

The second part of the experimental application of the proposed method regards the early detection and identification of a bearing fault during a run-to-failure test.

5.1 Experimental setup

This part of the analysis has been carried out by using the vibration signals contained into a data set provided by the Center for Intelligent Maintenance Systems of the University of Cincinnati [15]. As shown by the scheme in figure 5, the test rig is composed by four bearings type Rexnord ZA-2115 mounted on the same shaft. During the test the rotational speed has been fixed at 2000rpm and a radial load of 27.7kHz has been applied to bearings 2 and 3. The vibration signals have been acquired through two accelerometers model PCB 253B33 mounted in radial direction. Each bearing has been monitored continuously acquiring 1s of signal each 10min with a sampling frequency of 20.48kHz. After 7 days the test has been stopped and an outer race fault has been detected in bearing 1.

5.2 Results

The target of this section is to demonstrate that the proposed criterion is able to monitor the progressive evolution of the bearing condition during the entire operative life in order to detect the appearance of faults as early as possible. For this scope, the variation of the maximized BD criterion during the endurance test can be observed taking account of three characteristic frequencies: the ball pass frequency outer race (BPFO), the ball pass frequency inner race (BPFI) and the ball spin frequency (BSF).

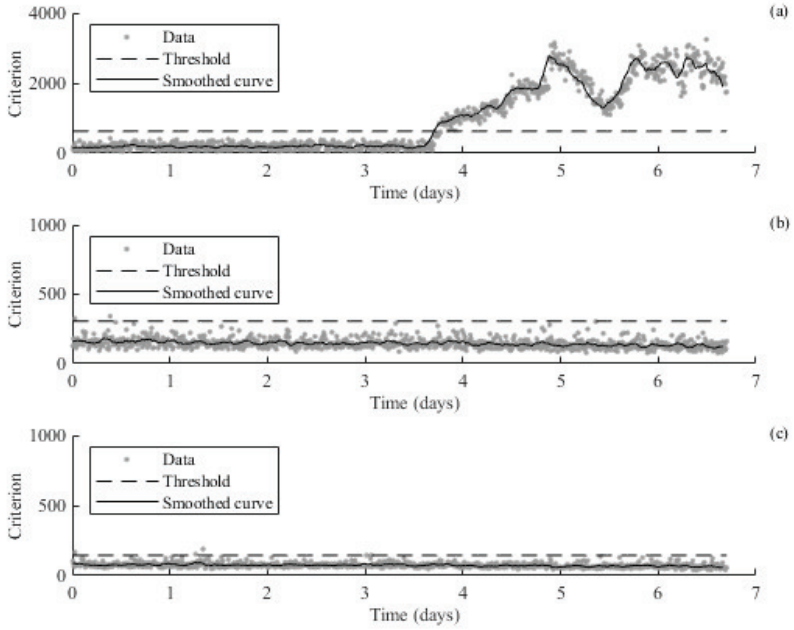

Figure 6: Final values of maximized criterion during the endurance test taking account of BPFO (a), BPFI (b) and BSF (c).

The FBBD method has been applied considering only the fundamental cyclic frequency related to the bearing fault and a 100 samples length FIR filter. Due to the experimental evidence, the analysis has been carried out considering only the faulty bearing 1.

Figure 6 collects the values of the maximized criterion calculated on bearing 1 during the endurance test. The figures depict a constant trend of values in the first stage of the test considering all the characteristic frequencies. However, in figure 6a it is possible to clearly identify an increasing trend starting after 3.7 days. This trend is not monotonically increasing but presents a decreasing trend between 5 and 5.5 days due to the characteristic propagation phenomena of the bearing fault [16].

The identification of the fault appearance can be obtained by designing a statistical threshold starting from the trend of the maximized values during the test. In this direction the values obtained are compared in figure 6 with a statistical threshold computed according to the Tukey's method applied on the values estimated in the first day of test, under the hypothesis that in this time span the system presents healthy condition. It is possible to observe in figure 6 that, accordingly to the experimental evidence on the physical system, only the trend of values related to the BPFO crosses the threshold after 3.8 days.

However, some values related to the BPFI and the BSF cross the respective threshold due to the dispersion of the BD criterion also in the healthy stage. This issue can be overcome by smoothing the values of the maximized criterion in order to make the data interpretation easier and to permit the identification of the time instant related to the fault appearance in a clearer way. The smoothed curves shown in figure 6 have been calculated exploiting the moving average technique implemented by convolving the BD final values series with a 15 samples length rectangular window. From the observation of the smoothed curves it is possible to note that only the trend related to the BPFO crosses the threshold and this behaviour confirms what has been detected experimentally on the studied system.

This application on a real case explains the sensitivity of the proposed BD criterion to the presence of cyclostationary patterns inside vibrational signals. This characteristic makes the FBBD algorithm suitable for the online monitoring of the bearing conditions during the overall operative life. A particular attention has to be pointed out on the number of cyclic frequencies considered; in fact the entire analysis has been carried out with the only cyclic frequencies α related to the specific fault, without consider any harmonics.

These results agree with the analysis proposed in Ref. [10] where the fault has been identified through the application of the CYCBD method also considering the harmonics of the cyclic frequency. The results prove

the effectiveness of the proposed method that is able to identify the fault appearance considering only the first cyclic frequency , although in this way the reconstruction quality of the estimated source may be not sufficient, as demonstrates in the previous section.

6 Final remarks

This paper presents a novel BD method based on the maximization of the cyclostationary behaviour of the signal. The proposed method exploits the Fourier-Bessel series expansion in order to rewrite the Indicator of Ciclostationarity and define a new BD criterion. The choice of the Fuorier-Bessel transform instead of the classic Fourier transform is related to the decay of the Bessel functions within the range defined by the length of the acquired signal. Thus, the impulsive signal can be reconstructed with a lower number of coefficient with respect to the Fourier transform based on sinusoidal functions.

The proposed algorithm, called FBBD, has been validated by means of both simulated and real signals in order to demonstrate the improvement given with respect to the other BD method based on cyclostationarity maximization, called CYCBD, in particular in term of lower computational time.

The application on simulated signal proves the lower number of cyclic frequencies required by the FBBD algorithm with respect to the CYCBD (70% less) according to the theoretical properties of the two different transform. The main issue is related to the inability of the FBBD to deconvolve the correct sign of the impulses; in fact the proposed method extracts an impulsive pattern composed by zero mean impulses, i.e. symmetric with respect to the zero, with the correct period and relative amplitude between the peaks.

The analysis of a run-to-failure test demonstrates the effectiveness of the proposed method for the continuous monitoring of the bearing conditions, in order to detect the fault appearance and to describe the progressive damage of the system. The proposed criterion proves to be very sensitive to the appearance of a cyclostationary source inside the signal, considering only the cyclic frequencies related to the fault, without its harmonics.

All these results demonstrate the clear improvement given by the proposed method that combines the suitability of the cyclostationarity for the description of vibrational signal related to bearing faults with the speed up of the iterative algorithm obtained through the exploitation of the Fourier-Bessel series expansion for the definition of the new BD criterion.

Acknowledgments

For the experimental validation presented in this work the dataset provided by the Center for Intelligent Maintenance Systems (IMS), University of Cincinnati has been used. Part of the analysis has been performed by using the code within Blind Deconvolution based on cyclostationarity maximization pack and provided by Marco Buzzoni.

References

[1] R.A. Wiggins *Minimum entropy deconvolution.* Geoexploration 16, n. 1-2, (1978), pp. 21-35.

[2] H. Endo, R.B. Randall *Enhancement of autoregressive model based gear tooth fault detection technique by the use of minimum entropy deconvolution filter.* Mechanical Systems and Signal Processing 21, (2007), pp. 906-919.

[3] L. Zhang, N. Hu *Fault diagnosis of sun gear based on continuous vibration separation and minimum entropy deconvolution.* Measurement 141, (2019), pp. 332-344.

[4] N. Sawalhi, R.B. Randall, H. Endo *The enhancement of fault detection and diagnosis in rolling element bearings using minimum entropy deconvolution combined with spectral kurtosis.* Mechanical Systems and Signal Processing 21, n. 6, (2007), pp. 2616-2633.

[5] G. McDonald, Q. Zhao, M. Zuo *Maximum correlated Kurtosis deconvolution and application on gear tooth chip fault detection.* Mechanical Systems and Signal Processing 33, (2012), pp. 237-255.

[6] G. McDonald, Q. Zhao *Multipoint Optimal Minimum Entropy Deconvolution and Convolution Fix: Application to vibration fault detection.* Mechanical Systems and Signal Processing 82, (2017), pp. 461-477.

[7] R.B. Randall, J. Antoni *Rolling element bearing diagnostics-A tutorial.* Mechanical Systems and Signal Processing 25, n. 2, (2011), pp. 485-520.

[8] J. Antoni *Cyclostationarity by examples.* Mechanical Systems and Signal Processing 23, n. 4, (2009), pp. 987-1036.

[9] M. Buzzoni, E. Soave, G. D'Elia, E. Mucchi, G. Dalpiaz *Development of an indicator for the assessment of damage level in rolling element bearings based on blind deconvolution methods.* Shock and Vibration 2018, (2018).

[10] M. Buzzoni, J. Antoni, G. D'Elia *Blind deconvolution based on cyclostationarity maximization and its application to fault identification.* Journal of Sound and Vibration 432, (2018), pp. 569-601.

[11] A. Raad, J. Antoni, M. Sidahmed *Indicators of cyclostationarity: Theory and application to gear fault monitoring.* Mechanical Systems and Signal Processing 22, (2008), pp. 574-587.

[12] R.B. Pachori, P. Sichar *A new technique to reduce cross terms in the Wigner distribution.* Digital Signal Processing 17, (2007), pp. 466-474.

[13] A. Bhattacharyya, L. Singh, R.B. Pachori *Fourier-Bessel series expansion based empirical wavelet transform for analysis of non stationary signals.* Digital Signal Processing 78, (2018), pp. 185-196.

[14] J. Schroeder *Signal processing via Fourier-Bessel series expansion.* Digital Signal Processing 3, (1993), pp. 112-124.

[15] J. Lee, H. Qiu, G. Yu, J.Lin *Rexnord Technical Services, Bearing Data Set, IMS, University of Cincinnati, NASA Ames Prognostics Data Repository.* , 2007. url: http://ti.arc.nasa.gov/project/prognostic-data-repository.

[16] T. Williams, X. Ribadeneira, S. Billington, T.Kurfess *Rolling element bearing diagnostics in run-to-failure lifetime testing.* Mechanical Systems and Signal Processing 15, (2001), pp. 979-993.